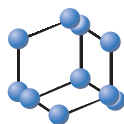


RESEARCH ARTICLE

BENTHAM
SCIENCE

In Vivo Performance of a Ruthenium-cyclopentadienyl Compound in an Orthotopic Triple Negative Breast Cancer Model



Nuno Mendes^{a,b}, Francisco Tortosa^c, Andreia Valente^d, Fernanda Marques^e, António Matos^f, Tânia S. Morais^d, Ana Isabel Tomaz^d, Fátima Gärtner^{a,b,g} and M. Helena Garcia^{d,*}

^ai3S-Instituto de Investigação e Inovação em Saúde, Universidade do Porto, Portugal; ^bIpatimup-Instituto de Patologia e Imunologia Molecular da Universidade do Porto, Portugal; ^cInstituto de Anatomia Patológica, Faculdade de Medicina da Universidade de Lisboa, Av. Prof. Egas Moniz, 1649-028 Lisboa, Portugal and Departamento de Medicina, Universitat Autònoma de Barcelona (UAB), Barcelona, Spain; ^dCentro de Química Estrutural, Faculdade de Ciências da Universidade de Lisboa, Campo Grande, 1749-016 Lisboa, Portugal; ^eCentro de Ciências e Tecnologias Nucleares, Instituto Superior Técnico, Universidade de Lisboa, Estrada Nacional 10 (km 139.7) 2695-066 Bobadela LRS, Portugal; ^fCiiEM-Centro de Investigação Interdisciplinar Egas Moniz, Campus Universitário, Quinta da Granja, Monte de Caparica, 2829-511 Caparica, Portugal and Centro de Estudos do Ambiente e do Mar (CESAM/FCUL)-Faculdade de Ciências da Universidade de Lisboa, Campo Grande, 1749-016 Lisboa, Portugal; ^gICBAS-Instituto de Ciências Biomédicas de Abel Salazar, Universidade do Porto, Portugal

Abstract: Background: Ruthenium-based anti-cancer compounds are proposed as viable alternatives that might circumvent the disadvantages of platinum-based drugs, the only metalodrugs in clinical use for chemotherapy. Organometallic complexes in particular hold great potential as alternative therapeutic agents since their cytotoxicity involves different modes of action and present reduced toxicity profiles.

Objective: During the last few years our research group has been reporting on a series of organometallic ruthenium(II)-cyclopentadienyl complexes with important cytotoxicity against several cancer cell lines, surpassing cisplatin in activity. We report herein preliminary *in vivo* studies with one representative compound of this family, with exceptional activity against several human cancer cell lines, including the glycolytic and highly metastatic MDAMB231 cell line used in this study.

Method: The anti-tumor activity of our compound was studied *in vivo* on N:NIH(S)II-nu nude female mice bearing triple negative breast cancer (TNBC) orthotopic tumors. Administration of 2.5 mg/kg/day during ten days caused cell death mostly by necrosis (*in vitro* and *in vivo*), inducing tumor growth suppression of about 50% in treated animals when compared to controls.

Results: The most remarkable result supporting the effectiveness and potential of this drug was the absence of metastases in the main organs of treated animals, while metastases were present in the lungs of all control mice, as revealed by histopathological and immunohistochemical analysis.

Conclusion: These *in vivo* studies suggest a dual effect for our drug not only by suppressing growth at the primary tumor tissue but also by inhibiting its metastatic behavior. Altogether, these results represent a benchmark and a solid starting point for future studies.

ARTICLE HISTORY

Received: March 31, 2016
Revised: July 12, 2016
Accepted: September 16, 2016

DOI:
10.2174/18715206166661609221651
33

Keywords: Ruthenium-cyclopentadienyl, triple-negative breast cancer, metastases, metaldrug, anti-cancer.

INTRODUCTION

Cancer describes over 100 disease conditions that share several common hallmarks. Despite prevention, early detection, and novel therapies, cancer is still the second leading cause of death in developed countries. According to the World Health Organization, the number of worldwide deaths from cancer is projected to rise to over 13.1 million people in 2030 [1]. Breast cancer (BC) in particular is the most prevalent type of cancer diagnosed among women. Despite advances in the prevention, early detection and treatment, BC remains the leading cause of cancer deaths in women worldwide [2]. Among the different subtypes of BC, triple negative BC (TNBC), defined by being negative for estrogen receptor alpha (ERα-), progesterone receptor (PR-) and human epidermal growth factor receptor 2 (HER2-), is responsible for a high mortality rate

and accounts for 15-20% of all BC cases among women [3, 4]. These tumors are characterized by being highly aggressive, having an elevated risk of recurrence and a high metastatic potential resulting, in most cases, in early death [5]. Variations in morphology and biologic characteristics result in different clinical and therapeutic outcomes. Whereas hormone receptor positive BCs have favorable responses to chemotherapy and targeted therapy treatment, TNBC has no directed therapy and no effective treatment protocol has been standardized [6-8]. Improvement of TNBC treatments has been using association of different drugs that only lead to a short time improvement in the survival rate (3.6 months) [9-14] with the inconvenience of severe side effects. TNBC chemotherapies have mainly been based in anthracyclines [8] or taxanes regimens followed by radiation and surgery. Refinement of TNBC treatments have been using association of taxanes with cisplatin and carboplatin (effective against several cancers e.g. lung, ovarian). [9-14] All these anticancer drugs reveal serious problems associated to their non-differentiated cytotoxicity, causing nausea, vomiting, and alopecia deepened by other major toxicities (e.g. cardiotoxicity, myelosuppression, among other effects). To overcome the

*Address correspondence to this author at the Centro de Química Estrutural, Faculdade de Ciências da Universidade de Lisboa, Campo Grande, 1749-016 Lisboa, Portugal; Tel: +351 217500972; Fax: +351 218500088; E-mail: mhgarcaia@fc.ul.pt

inefficiency of classical chemotherapeutics (mechanisms centered in DNA and microtubules damage) other approaches have been considered, without significant success, using drug inhibitors for specific targets such as: i) angiogenesis inhibitors (slow the growth of new blood vessels) or ii) inhibitors of tyrosine kinase and PARP (poly ADP ribose polymerase) enzymes.

The dramatic negative impact that cancer diseases have in the human health and the lack of solutions for some of these conditions conveys urgency to the search of new and more effective drugs than those currently in clinical use. The lack of results involving drugs acting on DNA, cell microtubules, angiogenesis and enzyme functions supports the search for alternative structures to originate different mechanisms of action.

In the search of new metal-based therapeutic drugs for cancer treatment, ruthenium derivatives emerged as serious potential alternatives to platinum(II)-based pharmaceuticals, the only metallo-drugs approved worldwide in cancer therapy. In fact, ruthenium compounds are expected to suppress the major drawbacks associated to platinum based drugs, namely (i) severe toxicities and (ii) limited efficacy for a narrow range of tumors, as several of them exhibit inherent or acquired resistance [15-17]. Importantly, ruthenium derivatives may also display reduced toxicity against healthy tissues by binding to serum proteins [18-21]. Although some of the ruthenium compounds reported in the literature are considered to present modes of action analogous to that of cisplatin, for which DNA was found as the main target [22-26], their structural diversity can lead to alternative modes of action and other targets besides DNA. In fact, production of reactive oxygen species [27], inhibition of kinases [28, 29], modification of enzymatic activities [30] or redox reactions [31] are examples of different paths that have been suggested to be involved in the mode of action of ruthenium compounds with different mechanisms of action.

Among these ruthenium-based agents, the inorganic ruthenium(III) drugs NAMI-A and KP1019 have proceeded into clinical trials (phase I and preliminary phase II trials in patients). Their chemical instability in aqueous media is however a major drawback for drug formulations, and limited solubility has hindered dose escalation of KP1019 precluding its progress in phase II clinical trials [32].

Our studies concerning a new family of organometallic ruthenium-cyclopentadienyl ("RuCp") based compounds [33-38] revealed that their interaction with cell membrane, the Golgi apparatus and mitochondria can be on the basis of their cytotoxic effect [33, 34, 36]. Most of these compounds have bidentate ligands bound to the ruthenium fragment *via* heteroatoms (N, N), (N, O), (N, S) that confer stability to the complexes enhancing their biological activity. Among these compounds we recently found an exceptional cytotoxic activity for TM90, $[\text{Ru}(\eta^5\text{-C}_5\text{H}_5)(\text{PPh}_3)(\text{bopy})][\text{CF}_3\text{SO}_3]$ (PPh_3 = triphenylphosphane; bopy = 2-benzoylpyridine) against breast cancer cell lines, both MCF7 and the highly glycolytic MDAMB231 cells, with IC_{50} values in the nanomolar range surpassing in great extent the activity of cisplatin [38]. To further extend our studies with TM90 and prospecting its value as a potential metallodrugs, assays in animal models are mandatory.

Towards this goal, the work herein presents our preliminary *in vivo* studies concerning the anticancer therapeutic effect of TM90 in an orthotopic TNBC mouse model. Due to the lack of an effective treatment in the clinic for triple negative breast cancer, cisplatin (used in combined chemotherapies to treat TNBC) was chosen as a positive control. Our studies also include the biodistribution of ruthenium through the main organs, blood and tumors, evaluation of the antimetastatic potential of TM90 and a preliminary evaluation of its toxicity (in terms of animals wellbeing, weight loss and lifetime extent).

MATERIALS AND METHODS

Ruthenium Compound

The ruthenium complex $[\text{Ru}(\eta^5\text{-C}_5\text{H}_5)(\text{PPh}_3)(\text{bopy})][\text{CF}_3\text{SO}_3]$ where PPh_3 is triphenylphosphane and bopy is 2-benzoylpyridine, abbreviated as TM90, was synthesized and purified under dinitrogen atmosphere using *Schlenk* techniques as previously described [38]. TM90 chemical stability in aqueous media was studied in DMEM (the cellular media used in the *in vitro* assays and the vehicle used during *in vivo* studies) at room temperature for 3 days and at 37 °C during 48 h. A low amount of DMSO (2% v/v) was used to fully dissolve the complex for the concentrations needed for UV-Vis spectroscopy.

Cell Culture and Viability Assays

The highly invasive human TNBC cell line MDAMB231 was obtained from ATCC (American Type Culture Collection, Manassas, VA, USA). Cells were maintained in DMEM with Glutamax I (Gibco®) supplemented with 10% fetal bovine serum (FBS) and 1% penicillin/streptomycin, in a 5% CO_2 incubator (Heraeus, Germany) at 37 °C and humidified atmosphere. The cells were adherent in monolayers and upon confluence were harvested by digestion with trypsin-EDTA. Cell viability was evaluated using a colorimetric assay based on the tetrazolium salt MTT ([3-(4,5-dimethylthiazol-2-yl)-2,5-diphenyltetrazolium bromide]), which is reduced by a mitochondrial dehydrogenase in metabolic active cells to insoluble purple formazan crystals [39]. For this purpose, cells were plated in 96-well plates at $10\text{--}20 \times 10^3$ cells/200 μL . For 24 h cells were allowed to adhere followed by the addition of dilution series of the compounds, TM90 and cisplatin, in fresh medium in 200 μL aliquots. TM90 was first solubilized in DMSO and then in medium, and added to final concentrations ranging from 0.1 μM to 200 μM . The final concentration of DMSO in cell culture medium did not exceed 1%. At this concentration (1%) the effect of DMSO in cell proliferation was tested and found to have no cytotoxic effect. Cisplatin, used as positive control, was first solubilized in water and then added to the culture medium at the same final concentrations of the tested complex in the range 0.1-200 μM . After continuous exposure to the compounds for 3 h and 24 h at 37°C/5% CO_2 , the medium was discarded and cells were incubated with 200 μL of MTT solution in PBS (0.5 mg/mL). After 3 h at 37°C/5% CO_2 , the solution was removed and the purple formazan crystals formed inside the cells were dissolved in 200 μL DMSO. The cellular viability was evaluated by measuring the absorbance at 570 nm using a plate spectrophotometer (PowerWave Xs, Bio-Tek Instruments, Winooski, VT, USA). The cytotoxic effect of both compounds was quantified by calculating the drug concentration inhibiting tumor cell growth by 50% (IC_{50}), based on a non-linear regression analysis of dose response data (GraphPad Prism software).

Effect of HSA on the Cytotoxicity of Compounds

MDAMB231 cells were seeded on 96-well plates 24 h before incubation with the compounds in complete medium containing only 5% FBS. The reduction of FBS concentration was required in order to decrease the total protein content in the culture medium. Too high protein concentrations increase the viscosity of the medium, causes foaming and a decrease in cellular viability. The effect of human serum albumin (HSA) on cell viability of MDAMB231 cells, either alone or incubated with TM90 or cisplatin, was evaluated using the IC_{50} concentration of the compounds at 24 h. For that, compounds were pre-incubated for 20 min at 37 °C with different concentrations of HSA at compound-to-protein molar ratios of 1:0.5, 1:1 and 1:2, and then added to the cells. After a 24 h incubation period the treatment solutions were removed and the cellular viability was measured by the MTT assay.

Cell Death Measurement by Flow Cytometry

MDAMB231 cells were treated with the compounds at a concentration equivalent to their IC_{50} at 24 h incubation. After 24 h, cells (*ca.* 1×10^5) were harvested by centrifugation and washed twice with ice-cold phosphate-buffered saline (PBS). To determine the percentage of dead cells, the pellet was resuspended in binding buffer (0.01M Hepes pH 7.4, 0.14M NaCl, 2.5mM $CaCl_2$) containing propidium iodide (PI) and annexin V. After 20 min in the dark at room temperature, the rate of apoptotic and/or necrotic cells was measured by flow cytometry with a Beckman Coulter EPICS XL-MCL. All data were analyzed using WinMDI 2.9 software.

Animal Studies

Animal experiments were carried out in accordance with the European Guidelines for the Care and Use of Laboratory Animals, Directive 2010/63/UE and ethical approval was obtained from the Ethic Committee. N:NIH(S)II-*nu/nu* mice, strain described by Azar *et al.* [40] in 1980 were produced under the supervision of Ipatimup, housed and maintained at CIM-FMUP Animal House in a pathogen-free environment under controlled conditions of light and humidity. The following *Humane Endpoints* for euthanasia were established: i) any signals of distress, suffering or pain; ii) weight loss greater than 20-25% of the body mass; iii) anorexia and moribund state, related or not to the experimental procedure. In all experiments, mice aged 4-8 weeks old were used. As there is no effective TNBC treatment (usually patients are administered a mixture of drugs accordingly to their personal response to them), cisplatin, one of platinum drugs in clinical use for chemotherapy, was chosen as reference in this study. In all *in vivo* experiments, mice were monitored at least once a day.

Toxicological Studies

For this preliminary study doses were based on the IC_{50} value obtained for TM90. The *in vivo* toxicity was assessed in 6-8 weeks-old male N:NIH(S)II-*nu/nu* nude mice to evaluate both the lethal and the tolerated dose.

For TM90 the following doses were tested: 25.0, 12.5, 5.0 and 2.5 mg/Kg, per mice ($n = 3$ per group). Mice were intraperitoneally (IP) injected with a mixture of DMEM and DMSO in a proportion of 3:1 with each dose being administered every 24 h until animals showed signals of pain or distress.

For cisplatin 5.0 mg/Kg per mice ($n=4$ per group) was tested based on literature data [41-43]. Cisplatin was diluted in a saline buffered solution prior to administration. This dose was found to be toxic to the animals (N:NIH(S)II-*nu/nu* nude mice) and thus 2.5 mg/Kg was chosen as the treatment dose in order to better correlate the results with those from TM90 treatment.

Animal reaction to both TM90 and cisplatin was observed after injection and only stable animals proceeded to next dose. The effect of the treatment on the body weight was evaluated once per day.

Induction of Human Breast Tumors in Mice and Promotion of Metastasis

Female N:NIH(S)II-*nu/nu* mice, aged 4-6 weeks, were orthotopically inoculated with 2.5×10^6 viable MDAMB231 cells in the mammary fat pad using a 25 gauge needle. A total of 24 mice were inoculated. As soon as the nodules were visible (day 4), mice were randomized and divided into control ($n=7$, one animal did not show tumor development and was excluded from the study) and treatment group ($n=16$). The animals received either an IP injection of 100 μ L of DMEM/DMSO mixture (vehicle alone) in a proportion of 3:1 (control group) or a dose of 2.5 mg/Kg per animal

of TM90 (treatment group). After 10 consecutive days of treatment (day 13 in Fig. 1), the treated animals ($n=14$, two animals had to be excluded due to body weight loss at day 8 and day 11) were divided into two groups to which: i) group 1 ($n=8$) a maintenance dose of 1 mg/Kg per animal was given until days 25-26 and ii) group 2 ($n=6$) the treatment was ended. Tumor size was measured using calipers, and tumor volumes (mm^3) were estimated using the formula: $W \times L^2 \times \frac{1}{2}$, where W is the width and L is the length of the tumor. In order to extend mice life and promote metastatization, tumors of all mice groups were surgically removed when controls reached a mean volume of $\sim 2000-2500mm^3$ (days 24-26). Mice were anesthetized IP with 100 μ L of a mixture containing 50 mg/kg of Ketamin (IMALGENE 1000) and 1 mg/kg of medetomidine hydrochloride (Medetor[®]) to remove the tumor tissue. Whenever no local invasion was observed, a total excision of the tumors was performed. A dose of 2.5 mg/kg of atipamazole hydrochloride (Revertor[®]) per mice was used to revert the effect of anesthesia. Mice were treated with an oral solution of 10 mg/kg Tramal, every 8 h for 24-48 h to avoid pain. At the time of surgeries, organs were collected and fixed in 2% buffered glutaraldehyde for electron microscopy or 10% buffered formalin for histology.

For cisplatin a similar procedure was performed, *i.e.*, a total of 16 mice were used and divided in control and treatment groups ($n=8$ mice per condition). A dose of 2.5 mg/Kg of cisplatin was used, IP, per animal (treated group) for 5 days. After this period considerable weight lost was observed and considering animal's wellbeing the dose administered at days 6 and 7 was reduced to 1.25 mg/Kg and no further drug was given until day 10. At the end of this treatment cycle (day 11) the treated group was divided and a half ($n = 4$) continued the treatment with a maintenance dose of 1 mg/Kg of cisplatin per mice, while for the other half ($n = 4$) the

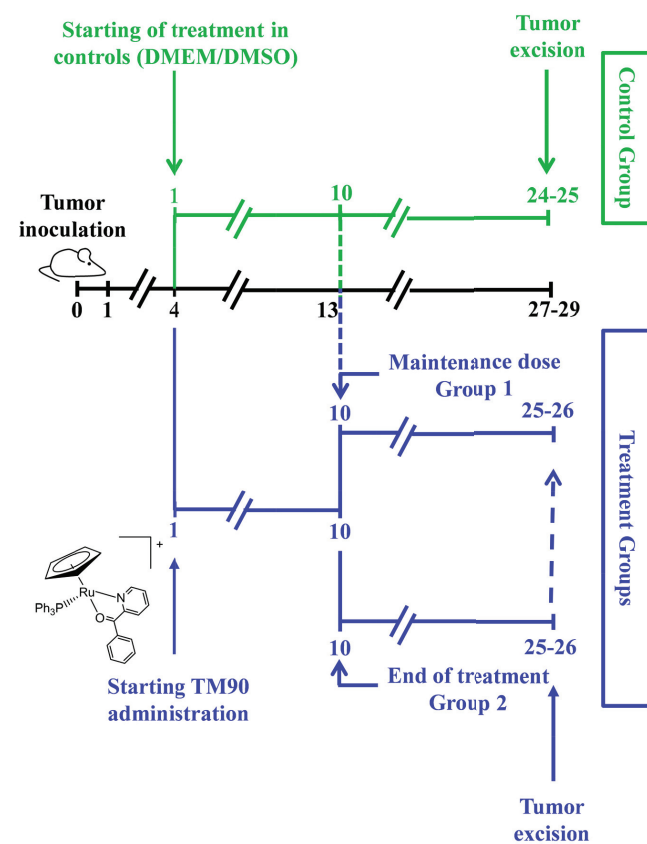


Fig. (1). Timeline showing tumor inoculation (day 0), beginning of treatment (at day 4) and tumor excision for control and treatment groups (days 27-29). The structure of TM90 is included (bottom left).

treatment was ended. As soon as the control tumors reached a volume of $\sim 2000 \text{ mm}^3$, all tumors were excised according to the protocol mentioned above.

After tumor excision in controls and treated groups (TM90 and cisplatin), mice were only euthanized when any of the established *Humane Endpoints* was observed in order to evaluate the possible formation of metastasis and the overall survival; necropsies were made in all animals.

Biodistribution of Complex in Mice Main Organs

The biodistribution of TM90 in mice was assessed in both healthy and tumor bearing animals. Healthy animals ($n = 2$) from the toxicological study were used after receiving a cumulative dose of 20 mg/Kg (administered along 7 days). Mice were anesthetized for whole venous blood collection by intracardiac puncture and then euthanized to collect heart, lung, liver and kidneys. After collection, the blood and the different organs were promptly frozen at -20°C .

From tumor xenografted animals ($n = 2$), the main metabolic organs (liver and kidneys) and tumors were also collected after receiving a cumulative dose of 20 mg/Kg. Tissue samples were washed in saline buffer solution, placed in plastic tubes and frozen for subsequent quantification of ruthenium by ICP-MS. Samples were lyophilized, weighted and digested with ultrapure HNO_3 , H_2O_2 and H_3PO_4 in a closed pressurized microwave digestion unit (Mars5, CEM) with medium pressure HP500 vessels and then diluted in ultrapure water to obtain 2.0% (v/v) nitric acid. Ruthenium content in the different organs was measured by a Thermo X-Series Quadrupole ICP-MS (Thermo Scientific). The instrument was tuned using a multi-element ICP-MS 71 C standard solution (Inorganic Venture). Indium (^{115}In) at 10 μM was used as internal standard.

Histopathological and Immunohistochemical Analysis

The specimens to analyze correspond to selected organs tissues (heart, lungs, liver, spleen and kidneys) and excisional biopsies of tumor tissue, previously implanted in the animal model. The tissues were fixed in buffered formalin and the inclusion in paraffin was done according to the usual technical procedures. Histological sections of 3 microns, stained with haematoxylin and eosin (H&E) and mounted on microscope slides were made. The slides were observed with an optical microscope (Nikon Eclipse 50i) and iconography microscopic images captured using a digital camera coupled (DS Camera Control Unit DS-L2). Histological evaluation was made in blind analysis by the pathologist. The samples were compared with those of control mice and histological variables as coagulation necrosis, intratumoral haemorrhage, lymphocytic infiltration, peritumoral oedema, peripheral pseudopalisading and vascular proliferation, as well as the degree of tumor regression were evaluated. The quantification of the number of mitoses was performed by counting ten fields of high magnification (10HPF) of the tumor periphery and the mean of this count was used as mitotic index. Immunohistochemical studies were performed on paraffin-embedded tumor tissue, following the usual technical procedures for each marker. All animals in the control group were used to guarantee the reliability and reproducibility of the results. For each sample, Phosphohistone-H3 antibody (PHH3; Cell Marque; 1:100) was used to aid in quantifying the number of mitoses (counting cellular immunostain in 10HPF); the tumor cell proliferation was assessed by the percentage of positive nuclei for Ki-67 (proliferative index, Ab-4; Thermo Scientific; 1:300) in 500-1000 tumor cells, analysed under an optical microscope at high magnification ($\times 400$). Regulation of CD52 (caspase-3, Cpp32; DCS; 1:200) to study cell apoptosis was also studied (it was calculated as the percentage of neoplastic cells with cytoplasm immunoreactivity, in at least in 500 tumor cells, analyzed in light microscope with $\times 400$ magnification).

Ultrastructural Studies by Transmission Electron Microscopy (TEM)

Samples from the tumor mass from treated and non-treated animals which did not display macroscopic necrotic changes, were cut in fragments of less than 1 mm^3 and fixed in 3% glutaraldehyde in 0.1 M cacodylate buffer pH 7.3, followed by 1% osmium tetroxide in the same buffer and uranyl acetate 0.5% in acetate acetic acid buffer 0.1M, pH 5.0. After dehydration in ethanol and passage in epoxypropane, the samples were embedded in an Epon-Araldite mixture. One micrometer sections and ultrathin sections were made with glass and diamond knives, respectively. One micrometer sections were stained with toluidine blue and ultrathin sections were contrasted with uranyl acetate and lead citrate; sections were examined and photographed in a JEOL 1200EX transmission electron microscope.

RESULTS AND DISCUSSION

Organometallic complexes are important alternative therapeutic agents to platinum based drugs in clinical use, since their cytotoxicity involves different modes of action and present reduced toxicity profiles. Our research group has been reporting during the last years a series of organometallic ruthenium(II)-cyclopentadienyl derived complexes that showed important cytotoxicity against several cancer cell lines, surpassing cisplatin in activity. Under this prospective, TM90 was our chosen compound to pursue to animal experiments due to its exceptional cytotoxicity against MCF7 and MDAMB231 human breast cancer cell lines.

TM90 Stability in Solution

Compound stability is an important feature that needs to be considered. One of the main problems associated with other promising ruthenium metallodrugs, such as NAMI-A and RAPTA-C, has been their short half-lifetimes [44, 45]. TM90 stability was evaluated by UV-Vis spectroscopy in DMEM cellular medium containing 2% DMSO at room temperature and 37°C . The composition of this medium was chosen to mimic as much as possible the conditions used in the *in vitro* studies with cancer cells and those used in the *in vivo* administration (with DMSO being used as a vehicle). TM90 was found to have a half-life time at room temperature of over 3 days (see Fig. 2) and of $\sim 17 \text{ h}$ at 37°C showing a considerable stability in these conditions.

TM90 Inhibits the Growth of MDAMB231 Cells in Culture-Cytotoxicity *in vitro*

We reported previously the cytotoxic activity of TM90 at 72 h ($\text{IC}_{50} = 0.03 \pm 0.01 \mu\text{M}$) [38]. In the present study, the IC_{50} value at 3 h and 24 h was determined in order to select the most appropriate incubation time and concentration for the studies with HSA and for apoptosis in MDAMB231 cells. Cisplatin was used as the positive control. For this purpose, cells were treated with increasing concentrations of TM90 and cisplatin in the range 0.1-200 μM . As shown in Fig. 3A the half maximal inhibitory concentration values at 3 and 24 h were respectively $6.66 \pm 3.5 \mu\text{M}$ and $0.73 \pm 0.12 \mu\text{M}$ for TM90 and $241 \pm 140 \mu\text{M}$ and $104 \pm 16 \mu\text{M}$ for cisplatin (Dose-response curves are presented in Fig. S1).

Effect of HSA on the Cytotoxicity of TM90

The evaluation of binding to serum proteins is a requirement of the FDA as part of the drug development process. Considering that a vast majority of therapeutic metal-containing compounds is administered intravenously, binding toward serum proteins is determinant for their bioavailability. Given its high concentration in the blood stream, human serum albumin (HSA) in particular can act as a transport vehicle of metal drugs and can determine the overall

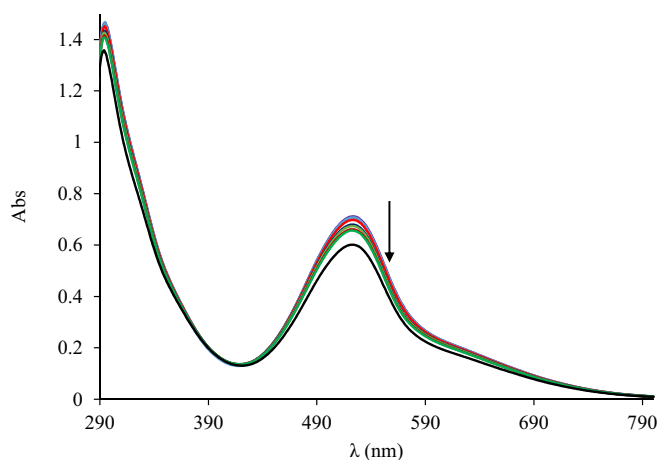


Fig. (2). Optical spectra of compound TM90 (at $\sim 1 \times 10^{-4}$ M) in DMEM with 2% DMSO studied with time evolution, $t = 0$ to $t = 24$ h at room temperature. The arrow indicates the variation of the characteristic MLCT band.

drug distribution and excretion, as well as differences in efficacy, activity and toxicity.

Given our previous results, TM90 forms an adduct with HSA with a binding constant comparable to that of KP1019 [46], which is known to be efficiently transported by albumin in the blood. The effect of the adducts formed between TM90 or cisplatin with HSA on the viability of MDAMB231 cells was evaluated at the IC_{50} (24 h) concentration for both compounds tested alone (1 μ M and 100 μ M, for TM90 and cisplatin, respectively). Results in Fig. 3B showed that both complexes preserve their cytotoxic activity when combined with HSA. This result together with our previous study on the interaction of TM90 with HSA for which a moderate binding constant was obtained [46] indicates that the interaction between TM90 and HSA does not deactivate the compound and thus one can expect that this protein might be involved in the distribution and delivery of TM90 to the cancer cells as observed for other ruthenium agents [47, 48].

Mechanism of Cell Death Promoted by TM90 (Apoptotic Cell Analysis)

In order to infer about the mechanism of cell death induced by TM90 on MDAMB231 breast cancer cells, flow cytometric analysis of cells double stained for Annexin V and propidium iodide (PI) was used. The externalization of phosphatidylserine is one of the leading indicators of apoptosis. Annexin V presents a high affinity

to bind to phosphatidylserine and thus it can be used to identify cells in all stages of the programmed cell death [49]. Propidium iodide (PI) exclusively stains cells with a disrupted cell membrane, *i.e.*, unviable cells, and can be combined with Annexin V to identify late apoptotic and dead cells. Finally, cells entering early apoptosis display phosphatidylserine (PS) exposure on the outer surface of the plasma membrane, which can be detected using Annexin V combined with PI [50, 51]. Viable cells are both Annexin V and PI negative. In this frame, the majority of control cells stained negative for both PI and Annexin V, indicating that they were mostly viable ($\sim 94\%$). Cells treated with TM90 (at the IC_{50} value at 24 h) showed a major population of necrotic cells (Annexin V⁺PI⁺) and a smaller population of late apoptotic cells (Annexin V⁺PI⁻), revealing that necrosis is the main cell death mechanism caused by TM90 (Fig. 4). In contrast, the control cisplatin (at a concentration equivalent to the IC_{50} value at 24 h challenge) presented a larger percentage of apoptotic cells (22% apoptotic vs. 5% necrotic), as reported previously [52].

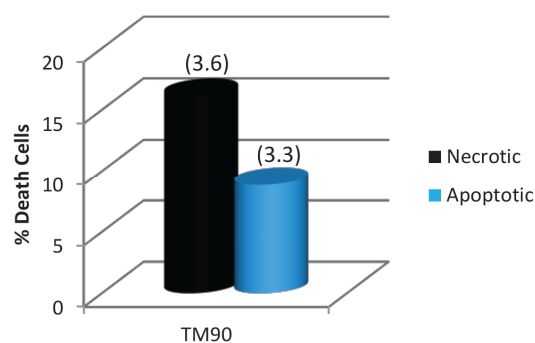


Fig. (4). Mechanism of cell death determined by flow cytometric analysis of MDAMB231 breast cancer cells, treated for 24 h at IC_{50} values of TM90. Apoptotic cells include both early and late apoptosis. Data in parentheses are (\pm SD).

Determination of Lethal and Tolerated Doses *in vivo*

For this preliminary evaluation the acute toxicity of TM90 was assessed in male N:NIH_(S)II-*nu/nu* mice with the aim to determine the lethal and the tolerated doses. For that purpose 4 groups of 3 male nude mice were used to which the following doses of TM90 were given: 25.0, 12.5, 5.0 and 2.5 mg/Kg, respectively to each group. Karber's method [53] was used to estimate LD_{50} value for TM90 and 19.5 mg/Kg was established as the lethal dose. Data from this experiment also allowed establishing the tolerated TM90 dose to be used in the antitumor ability evaluation. Body weight

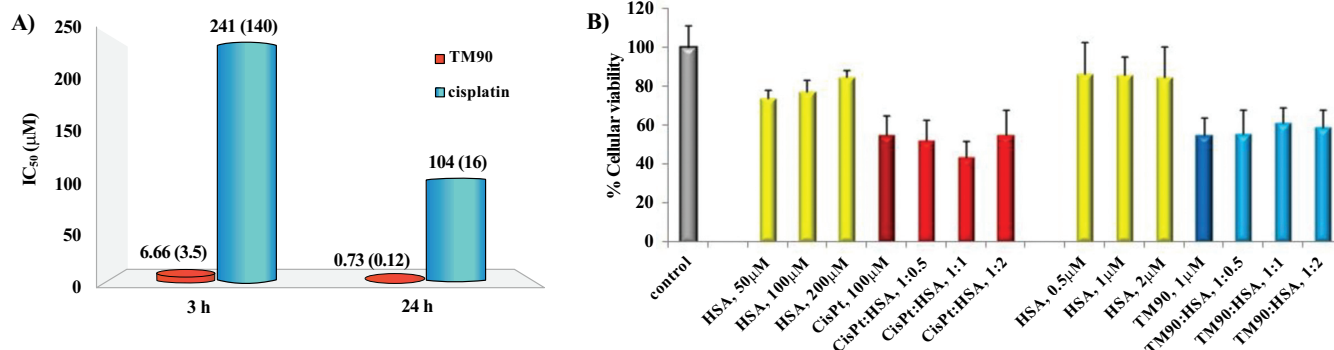


Fig. (3). A) IC_{50} values found for TM90 and cisplatin in the MDAMB231 cells at 3 h and 24 h treatment. B) Effect of HSA on the cytotoxicity of TM90 and cisplatin against the MDAMB231 cells after a 24 h challenge. Data: cells with no treatment (control); cells treated with HSA alone in the concentrations indicated; cells treated with the compounds in the absence of albumin at a concentration equivalent to the IC_{50} values; cells treated with compounds pre-incubated with albumin. Data shown are the mean values (\pm SD) of two independent experiments, performed with at least six replicates.

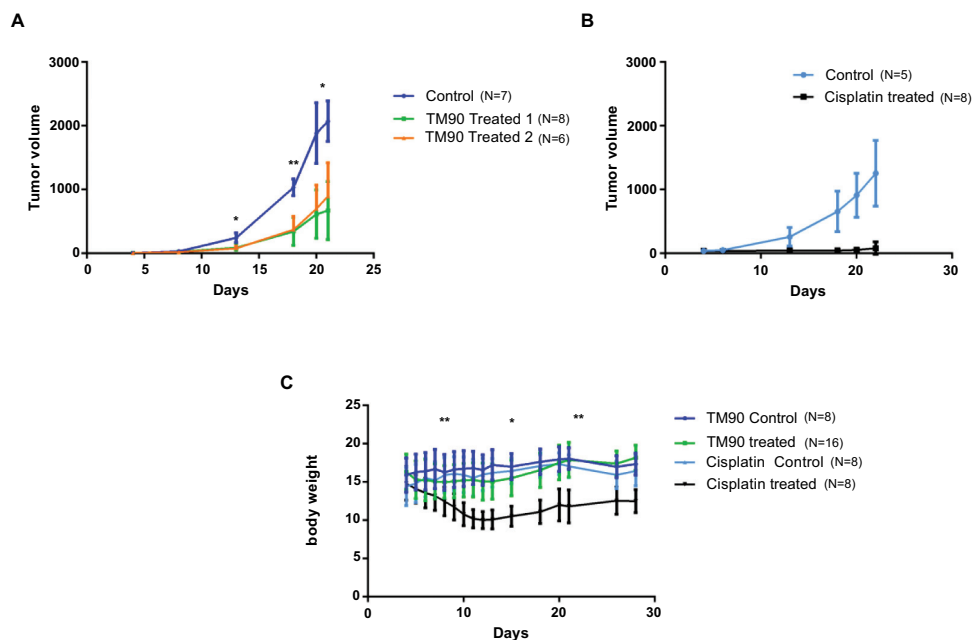


Fig. (5). A) Effect of TM90 in tumor volume evolution of MDAMB231 orthotopically inoculated in the mammary fat pad of N:NIH(S)II-nu/nu nude female mice. From day 4 to day 13, inclusively, treated group 1 and 2 were injected IP with 2.5 mg/Kg per animal of TM90. After day 13, treated group 1 maintained a 1 mg/Kg treatment until the excision of tumors (day 24). The number of animals used for each group is indicated on the figure. * $P < 0.0005$, compares untreated control with treated groups 2 at days 13, 20 and 21; ** $P < 0.0001$, compares untreated control with treated groups at day 18; B) Effect of cisplatin in tumor volume evolution. From day 3 to day 7, inclusively, treated group was injected IP with 2.5 mg/Kg of cisplatin. To maintain animal stability, the dose was reduced to 1.25 mg/Kg at days 8 and 9. After day 9 no more cisplatin was given; C) Effect of compounds in animal wellbeing, measured in terms of body weight. Body weight was measured once a day. No statistical significant values were obtained comparing control and TM90 treated animals. * $P \leq 0.0001$ change in body weight from day 8 to 3 between control and cisplatin treated animals. ** $P < 0.007$ change in body weight at days 8, 9, 26 and 28. The number of animals used for each group is indicated on the figure. P values were calculated using two-sided Student t-tests.

loss and the overall survival rate were found to be dose-dependent. A 2.5 mg/Kg dose was established as well tolerated by the animals, affording a stable body weight for at least 10 days of continuous administration with no apparent toxic symptoms.

In the case of cisplatin the continuous IP administration of 5.0 mg/Kg per day led to high toxicity and all mice had to be euthanized at day 8. For this reason 2.5 mg/kg was established as the treating dose mimicking the strategy performed for TM90.

In Vivo Anti-tumor Activity of TM90 on Female Mice Bearing TNBC Orthotopic Tumors

MDAMB231 TNBC cells were inoculated in the mammary fat pad of 4/6 weeks old [54, 55] female athymic nude mice ($n = 24$) as described in the experimental section. When tumor volumes reached the size of ~ 50 -100 mm³ mice were randomized and divided into groups (day 4, Fig. 1). The treated group started receiving an IP 2.5 mg/Kg per animal of TM90. Differences in the tumor volume between control and treated groups were visible after day 8 post-inoculation (Fig. 5A). At day 13, the 10 days cycle treatment was concluded and a statistically significant difference between untreated control and treated groups was observed ($P < 0.0005$). As shown on Fig. 5A, this difference was maintained even after the ending of the treatment. In order to better evaluate the differences in tumor volumes and to infer about other cancer aggressiveness properties, namely invasion and/or capacity to metastasize, treated animals were randomly divided into two groups at day 13. To Group 1, a maintenance dose of 1 mg/Kg of TM90 per day was administered until tumor surgical excision at days 25-26. To Group 2, no further TM90 was given. Fig. 6 shows a photographic comparison of the tumor size of untreated control and treated groups.

Differences between control and treated Groups 1 and 2 are shown on Fig. 5A and Fig. 6 and clearly demonstrate the *in vivo*

ability of TM90 in suppressing tumor growth over time (statistical differences between the two treated groups were not observed). Importantly, our data clearly show that, after surgical removal of the tumor, mice treated with TM90 present a significantly increased lifetime as shown on Fig. 7. Cisplatin also showed an important tumor suppression as shown in Fig. 5B.

Toxicity and animal wellbeing were evaluated in terms of body weight loss and relative overall survival. No differences in body weight were seen between mice treated with TM90 and the control group over time, showing that TM90 does not have a negative effect on animal wellbeing when compared with cisplatin (Fig. 5C). This result is also directly correlated with the overall survival of the animals (Fig. 6): TM90 treated mice lived longer than non-treated controls. To sum up, a dosage of 2.5 mg/Kg of TM90 per animal was effective and well tolerated, not presenting the severe side effects of the chemotherapeutic agent, cisplatin in this animal model.

Biodistribution of Complex in the Mice Main Organs

Information on TM90's biodistribution was obtained both on healthy and mice bearing tumors by quantitative analysis of ruthenium by ICP-MS. Considering healthy mice, blood and target organs (liver, lungs, kidneys and heart) were collected for animals that received a cumulative dose of 20 mg/Kg along 7 days. Results presented in Fig. 8 show that ruthenium was mainly accumulated in the liver, the central organ of metabolism, and in the kidneys. Lower accumulation was found in the heart, lungs and blood.

In what concerns tumor bearing animals, ruthenium content in the main metabolic organs (liver and kidneys) and tumors of two female animals treated with a cumulative dose of approximately 20 mg/Kg in a 7 days period was also quantified by ICP-MS. In this case high concentrations of ruthenium were also found in the liver

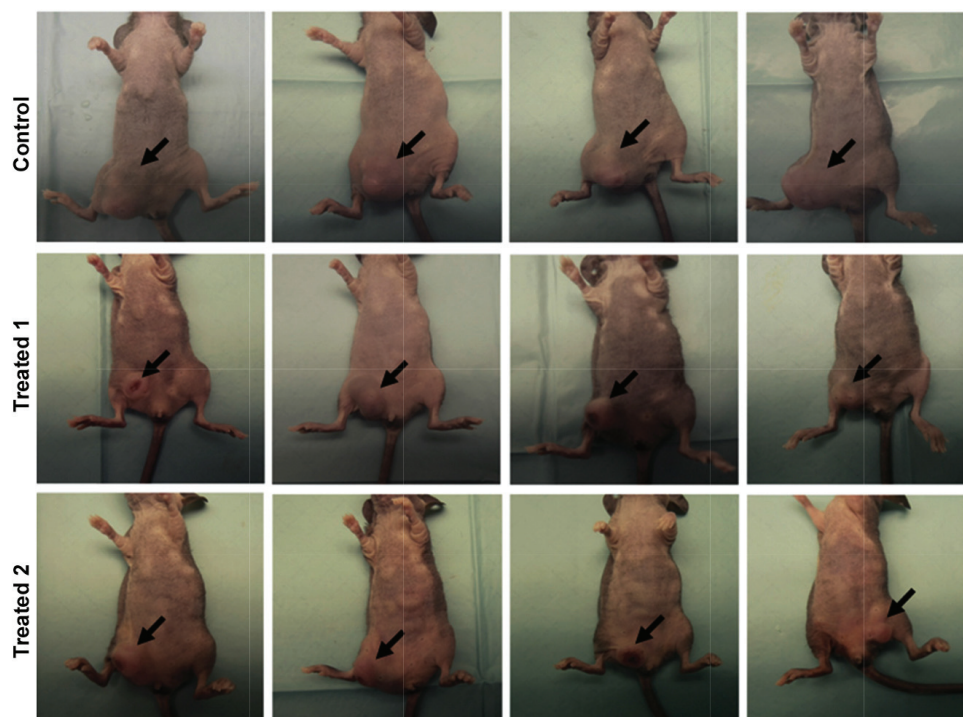


Fig. (6). Photographic comparison of the tumor size of untreated controls and treated groups. Photos taken at the days of surgeries, 4 animals per group are shown. Note that pictures of the treated groups were taken one or two days after those of the controls. Due to large number of animal subjects, surgeries could not be done at the same day.

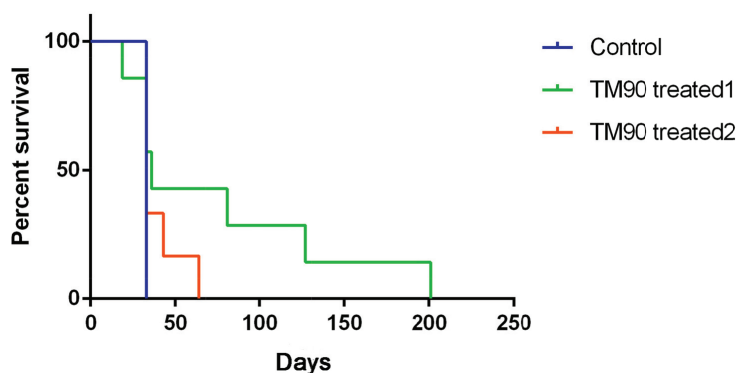


Fig. (7). TM90 Kaplan Meyer Survival Curve to compare overall survival among groups. Using a Mantel-Cox test a $P < 0.05$ was obtained when overall survival of mice in control group (in blue) was compared with overall survival of mice in treated group 1 (in green). In this analysis all animals in each group were used.

and kidneys. The ruthenium content in tumors was found to be very low (< 1 nmole Ru/g) compared with the main organs.

Even though these results cannot be directly compared due to the different metabolism that is sex dependent and to the different

TM90 is probably cleared from the blood and then excreted through the kidneys.

Histopathological and Immunohistochemical Analysis of Tumors and Organs and Ultrastructural Analysis by Transmission Electron Microscopy

Histopathological and immunohistochemical analysis of tumors and main organs was carried out. Tumor samples were compared with those of control mice and the histological variables analyzed, namely coagulation necrosis, intratumoral haemorrhage, lymphocytic

infiltration, peritumoral oedema, peripheral pseudopalisading and vascular proliferation, as well as the degree of tumor regression were evaluated. The number of mitoses was quantified as well. Significant differences between control and treatment groups were not observed, *i.e.* all mice tumors presented large necrotic regions, even though those from treated animals were considerably smaller. In the immunohistochemical study no changes on the PHH3 expression (average control tumors = 22/10HPF vs. average treated tumors = 26/10HPF) nor at the cellular proliferation index Ki-67 (average control tumors = 44% vs. average treated tumors = 41%) were observed. The caspase-3 immunostain was inconclusive due to the high degree of necrosis found in the tumors which hindered its clear reading and interpretation.

Transmission electron microscopy images of the tumor samples disclosed undifferentiated tumor cells with large nucleoli and highly irregular nuclei. Cytoplasmic organelles were scanty and

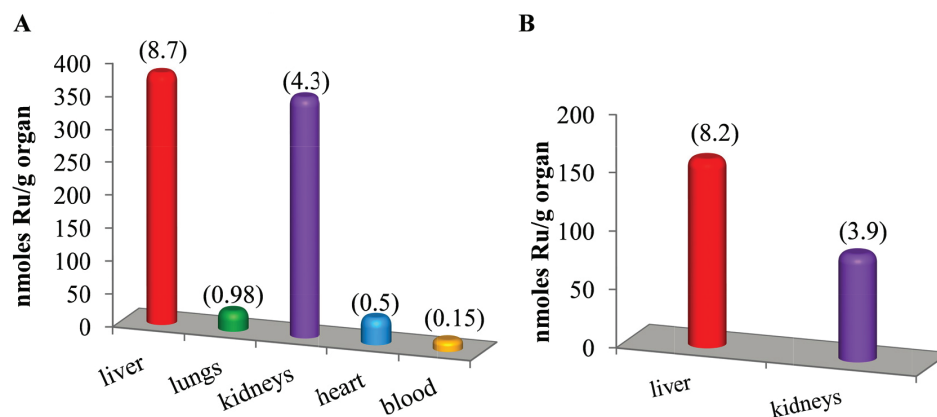


Fig. (8). Biodistribution of TM90 in mice main organs. (A) Ru content in blood and main organs of mice ($n = 2$) from the toxicological study after receiving a cumulative dose of TM90 (20 mg/kg) along 7 days. (B) Ru content in liver and kidneys of tumor xenograft mice ($n = 2$) after receiving a cumulative dose of TM90 (20 mg/kg) along 7 days. Data in parentheses are (\pm SD). Results were expressed as nmoles Ru/g of dry organ or tissue using ICP-MS analysis.

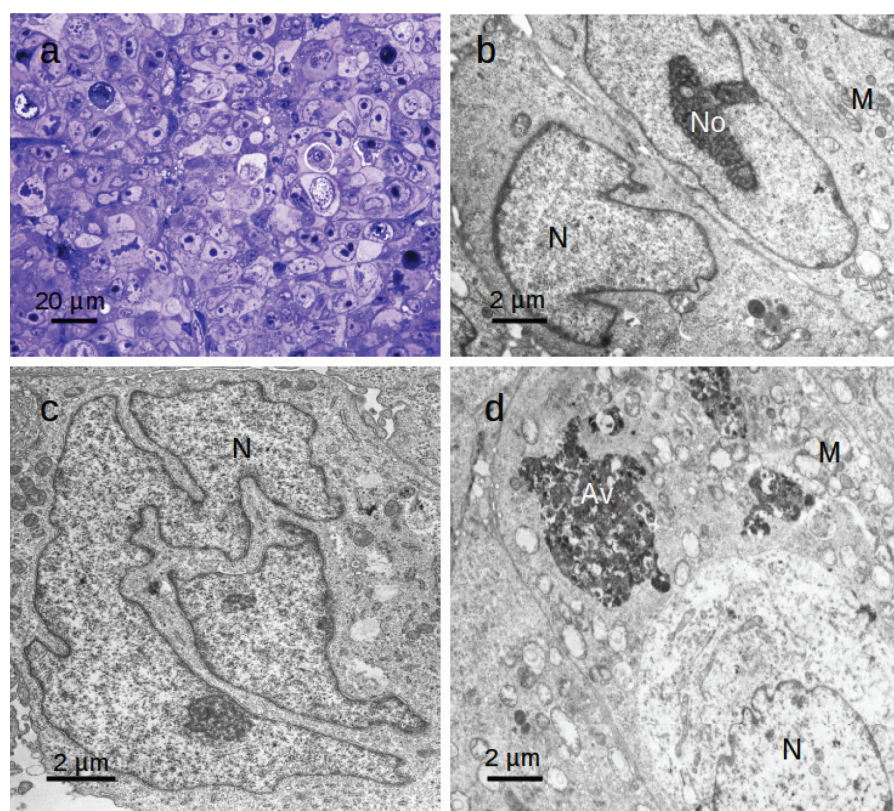


Fig. (9). TEM ultrastructural analysis of tumor cells from main mass of induced tumours. a) Toluidin blue stained 1 μ m section; b-d) Electron microscopy images showing organelles of undifferentiated cells. N – Nucleus; No – Nucleolus; M – Mitochondria; Av – Autophagic vacuoles.

occasional large autophagic vacuoles were observed. No significant ultrastructural differences were observed between treated and non-treated tumors (Fig. 9).

Since MDAMB231 tumors are known to induce metastasis mainly in lungs, this organ was carefully analyzed for all the controls and all treated groups (cisplatin and TM90). All control mice presented neoplastic cells in lungs, with one exception where the metastases were observed in a perirenal lymph node (Fig. 10A). Additional metastases were also found in the myocardium and liver for most of control mice (Fig. 10A).

As stated above, mice treated with TM90 were divided into two distinct groups. Concerning the mice treated during ten days with

2.5 mg/kg of TM90, followed by a maintenance dose until surgery removal (Group 1), only one of the four analyzed mice presented a small metastatic focus in the lungs. In Group 2, none of the mice presented metastases the organs analyzed: heart, lungs, liver, spleen and kidneys (Fig. 10B).

Cisplatin was used as a positive control and tumor regression was observed in all cases. Histopathological images of the lungs did not reveal the presence of metastases for most of the mice ($n = 3$). However, for one mouse, metastases were found in lungs, liver and spleen. In this case, carcinomatous lymphangioses and intra-parenchymatous tumor infiltration could be observed in the lungs (Fig. 10C).

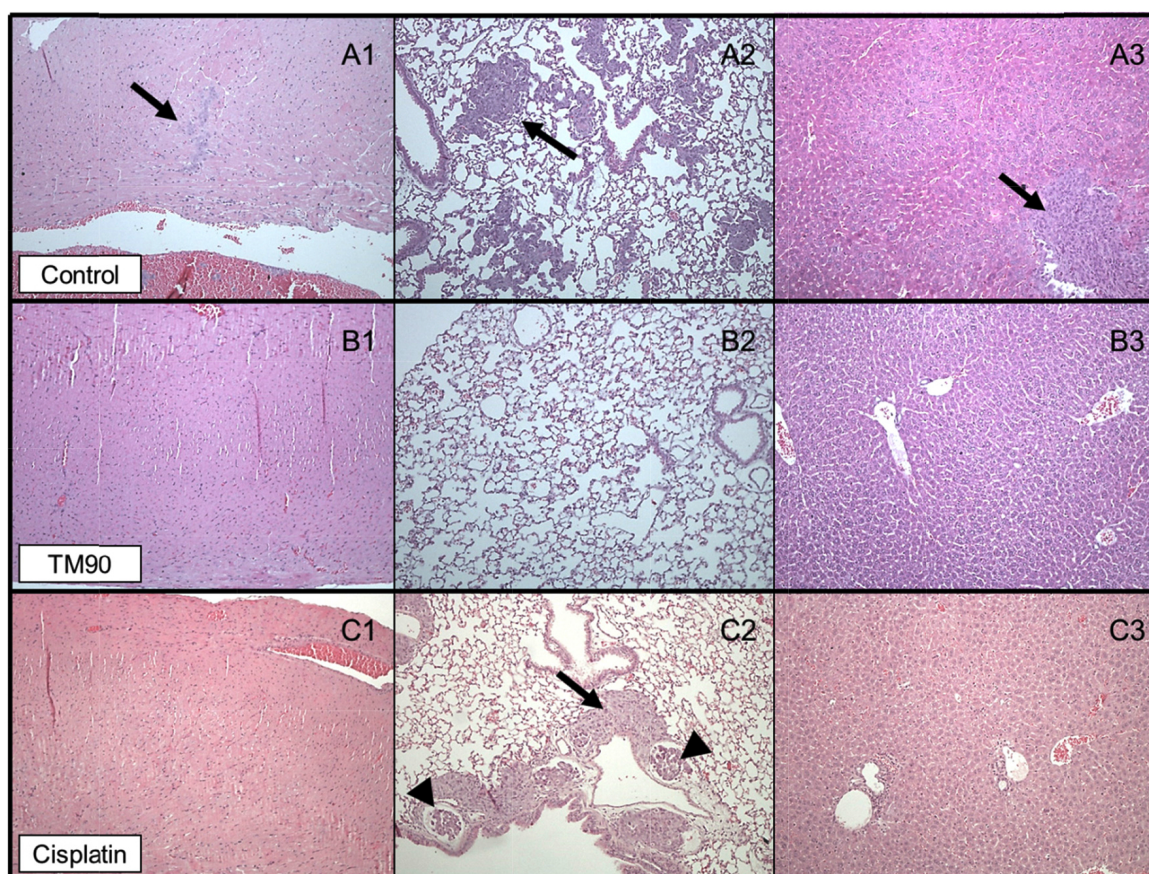


Fig. (10). A (control group): there is infiltration of tumor cells (arrows) in the myocardium (A1), lung (A2) and liver (A3); B (group treated with TM90): no metastasis (myocardium -B1-, lung -B2- and liver -B3-) was observed; C (group treated with cisplatin): this case do not show tumor cells in the heart (C1) or in the liver (C3); in the lung (C2) are observed carcinomatous lymphangioses (arrowhead) and intraparenchymal tumor infiltration (arrow) (H&E x100).

CONCLUSION

Studies involving the aggressive highly metastatic breast adenocarcinoma, carried out with a new cyclopentadienyl ruthenium derived compound, point out its great potential as metallodrug. It combines effectiveness against primary tumor tissue together with ability to suppress the development of metastases. This preliminary study is thus a benchmark for the “ruthenium-cyclopentadienyl” family of compounds as it brings these agents to the front stage on the search of new anticancer drugs.

SUPPLEMENTARY MATERIAL

Supplementary material is available on the publisher’s web site along with the published article.

CONFLICT OF INTEREST

The authors confirm that this article content has no conflict of interest.

ACKNOWLEDGEMENTS

This work was financed by national funds through FCT, the Portuguese Foundation for Science and Technology, within the scope of projects PTDC/QUI-QUI/118077/2010 and UID/QUI/00100/2013. Ana Isabel Tomaz and Andreia Valente thank the Investigator FCT2013 initiative for projects IF/01179/2013 and IF/01302/2013, respectively. Tânia S. Morais thanks FCT for her post-doctoral grant (SFRH/BPD/93513/2013). Authors thank to Ana Sofia Ribeiro and Catarina Gomes from Ipatimup for the support in the statistical analysis.

REFERENCES

- [1] The World Health Organization website. Available at: <http://www.who.int/mediacentre/factsheets/fs297/en/index.htm> (Accessed on January 2016).
- [2] Jemal, A.; Bray, F.; Center, M.M.; Ferlay, J.; Ward, E.; Forman, D. Global cancer statistics. *CA: Cancer J. Clin.*, **2011**, *61*(2), 69-90.
- [3] Lehmann, B.D.; Bauer, J.A.; Chen, X.; Sanders, M.E.; Chakravarthy, A.B.; Shyr, Y.; Pietenpol, J.A. Identification of human triple-negative breast cancer subtypes and preclinical models for selection of targeted therapies. *J. Clin. Investig.*, **2011**, *121*(7), 2750-2767.
- [4] De Laurentiis, M.; Cianniello, D.; Caputo, R.; Stanzone, B.; Arpino, G.; Cinieri, S.; Lorusso, V.; De Placido, S. Treatment of triple negative breast cancer (TNBC): current options and future perspectives. *Cancer Treat. Rev.*, **2010**, *36* Suppl 3, S80-S86.
- [5] Clemons, M.; Danson, S.; Howell, A. Tamoxifen (“Nolvadex”): A review. *Cancer Treat. Rev.*, **2002**, *28*(4), 165-180.
- [6] Liedtke, C.; Mazouni, C.; Hess, K.R.; André, F.; Tordai, A.; Mejia, J.A.; Symmans, W.F.; Gonzalez-Angulo, A.M.; Hennessey, B.; Green, M.; Cristofanilli, M.; Hortobagyi, G.N.; Pusztai, L. Response to neoadjuvant therapy and Long-Term survival in patients with triple-negative breast cancer. *J. Clin. Oncol.*, **2008**, *26*(8), 1275-1281.
- [7] Higgins, M.J.; Baselga, J. Targeted therapies for breast cancer. *J. Clin. Investig.*, **2011**, *121*(10), 3797-803.
- [8] Rabbani, A.; Davoodi, J. Effects of anthracycline antibiotic, daunomycin on thymus chromatin: The role of chromosomal proteins. *General Pharmacol. Vascular Syst.*, **1994**, *25*(4), 787-793.
- [9] Uhm, J.E.; Park, Y.H.; Yi, S.Y.; Cho, E.Y.; Choi, Y.L.; Lee, S.J.; Park, M.J.; Lee, S.H.; Jun, H.J.; Ahn, J.S.; Kang, W.K.; Park, K.; Im, Y.H. Treatment outcomes and clinicopathologic characteristics of triple-negative breast cancer patients who received platinum-containing chemotherapy. *Int. J. Cancer*, **2009**, *124*(6), 1457-1462.

- [10] Koshy, N.; Quispe, D.; Shi, R.; Mansour, R.; Burton, G.V. Cisplatin-gemcitabine therapy in metastatic breast cancer: Improved outcome in triple negative breast cancer patients compared to non-triple negative patients. *Breast (Edinburgh, Scotland)* **2010**, *19*(3), 246-248.
- [11] O'Shaughnessy, J.; Osborne, C.; Pippen, J.E.; Yoffe, M.; Patt, D.; Rocha, C.; Koo, I.C.; Sherman, B.M.; Bradley, C. Iniparib plus chemotherapy in metastatic triple-negative breast cancer. *New Engl. J. Med.*, **2011**, *364*(3), 205-214.
- [12] Mehta, R.S.; Schubert, T.; Jackson, D. Long-term outcome of phase II study of biweekly dose-dense AC followed by weekly paclitaxel and carboplatin and trastuzumab (TC ± H) based on HER2 status in large and inflammatory breast cancer (BC). *J. Clin. Oncol.*, **2010**, *28*(15s), Abstr 680.
- [13] Nieto, Y.; Shpall, E.J. High-dose chemotherapy for high-risk primary and metastatic breast cancer: Is another look warranted? *Curr. Opin. Oncol.*, **2009**, *21*(2), 150-157.
- [14] European Medicines Agency. Available at: http://www.ema.europa.eu/docs/en_GB/document_library/Summary_of_opinion_-_Initial_authorisation/human/000930/WC500014746.pdf (Accessed on February 2016).
- [15] Kelland, L. The resurgence of platinum-based cancer chemotherapy. *Nat. Rev. Cancer*, **2007**, *7*(8), 573-584.
- [16] Kannarkat, G.; Lasher, E.E.; Schiff, D. Neurologic complications of chemotherapy agents. *Curr. Opin. Neurol.*, **2007**, *20*(6), 719-25.
- [17] Markman, M. Toxicities of the platinum antineoplastic agents. *Exp. Opin. Drug Safety*, **2003**, *2*(6), 597-607.
- [18] Bruijninx, P.C.; Sadler, P.J. New trends for metal complexes with anticancer activity. *Curr. Opin. Chem. Biol.*, **2008**, *12*(2), 197-206.
- [19] Jakupec, M.A.; Galanski, M.; Arion, V.B.; Hartinger, C.G.; Keppler, B.K. Antitumor metal compounds: More than theme and variations. *Dalton Transact., (Cambridge, England: 2003)* **2008**, *2*, 183-194.
- [20] Dyson, P.J.; Sava, G. Metal-based antitumor drugs in the post genomic era. *Dalton Transact.*, **2006**, *16*, 1929-1933.
- [21] Allardyce, C.S.; Dyson, P.J. Ruthenium in medicine: Current clinical uses and future prospects. *Platinum Metals Rev.*, **2001**, *45*(2), 62-69.
- [22] Zeglis, B.M.; Pierre, V.C.; Barton, J.K. Metallo-intercalators and metallo-insertors. *Chem. Commun., (Cambridge, England)*, **2007**, *44*, 4565-4579.
- [23] Gill, M.R.; Derrat, H.; Smythe, C.G.W.; Battaglia, G.; Thomas, J.A. Ruthenium(II) Metallo-intercalators: DNA Imaging and Cytotoxicity. *Chem. Bio. Chem.*, **2011**, *12*(6), 877-880.
- [24] Metcalfe, C.; Thomas, J.A. Kinetically inert transition metal complexes that reversibly bind to DNA. *Chem. Soci. Rev.*, **2003**, *32*(4), 215-224.
- [25] Mei, H.Y.; Barton, J.K. Tris(tetramethylphenanthroline)ruthenium (II): A chiral probe that cleaves A-DNA conformations. *Proc. Nat. Acad. Sci. USA*, **1988**, *85*(5), 1339-1343.
- [26] Brabec, V. DNA Modifications by antitumor platinum and ruthenium compounds: Their recognition and repair. In *Progress in Nucleic Acid Research and Molecular Biology*, Academic Press: 2002; Vol. Volume 71, pp 1-68.
- [27] Jakupec, M.A.; Reisner, E.; Eichinger, A.; Pongratz, M.; Arion, V. B.; Galanski, M.; Hartinger, C.G.; Keppler, B.K. Redox-active antineoplastic ruthenium complexes with indazole: Correlation of *in vitro* potency and reduction potential. *J. Med. Chem.*, **2005**, *48*(8), 2831-2837.
- [28] Smalley, K.S.; Contractor, R.; Haass, N.K.; Kulp, A.N.; Atilla-Gokcumen, G.E.; Williams, D.S.; Bregman, H.; Flaherty, K.T.; Soengas, M.S.; Meggers, E.; Herlyn, M. An organometallic protein kinase inhibitor pharmacologically activates p53 and induces apoptosis in human melanoma cells. *Cancer Res.*, **2007**, *67*(1), 209-17.
- [29] Anand, R.; Maksimoska, J.; Pagano, N.; Wong, E.Y.; Gimotty, P. A.; Diamond, S.L.; Meggers, E.; Marmorstein, R. Toward the development of a potent and selective organoruthenium mammalian sterile 20 kinase inhibitor. *J. Med. Chem.*, **2009**, *52*(6), 1602-1611.
- [30] Ang, W.H.; De Luca, A.; Chapuis-Bernasconi, C.; Juillerat-Jeanneret, L.; Lo Bello, M.; Dyson, P.J. Organometallic ruthenium inhibitors of glutathione-S-transferase P1-1 as anticancer drugs. *Chem.Med.Chem.*, **2007**, *2*(12), 1799-806.
- [31] Dougan, S.J.; Habtemariam, A.; McHale, S.E.; Parsons, S.; Sadler, P.J. Catalytic organometallic anticancer complexes. *Proc. Nat. Acad. Sci.*, **2008**.
- [32] Bergamo, A.; Gaiddo, C.; Schellens, J.H.M.; Beijnen, J.H.; Sava, G. Approaching tumour therapy beyond platinum drugs: Status of the art and perspectives of ruthenium drug candidates. *J. Inorg. Biochem.*, **2012**, *106*(1), 90-99.
- [33] Morais, T.S.; Santos, F.; Corte-Real, L.; Marques, F.; Robalo, M.P.; Madeira, P.J.; Garcia, M. H. Biological activity and cellular uptake of [Ru(eta5-C5H5)(PPh3)(Me2bpy)][CF3SO3] complex. *J. Inorg. Biochem.*, **2013**, *122*, 8-17.
- [34] Corte-Real, L.; Matos, A.P.; Alho, I.; Morais, T.S.; Tomaz, A.I.; Garcia, M.H.; Santos, I.; Bicho, M. P.; Marques, F. Cellular uptake mechanisms of an antitumor ruthenium compound: the endosomal/lysosomal system as a target for anticancer metal-based drugs. *Microsc. Microanal.*, **2013**, *19*(5), 1122-1130.
- [35] Helena Garcia, M.; Morais, T.S.; Florindo, P.; Piedade, M. F.M.; Moreno, V.; Ciudad, C.; Noe, V. Inhibition of cancer cell growth by ruthenium(II) cyclopentadienyl derivative complexes with heteroaromatic ligands. *J. Ino. Biochem.*, **2009**, *10* (3), 354-361.
- [36] Morais, T.S.; Santos, F.C.; Jorge, T.F.; Corte-Real, L.; Madeira, P. J.; Marques, F.; Robalo, M.P.; Matos, A.; Santos, I.; Garcia, M.H. New water-soluble ruthenium(II) cytotoxic complex: Biological activity and cellular distribution. *J. Inorg. Biochem.*, **2014**, *130*, 1-14.
- [37] Tomaz, A.I.; Jakusch, T.; Morais, T.S.; Marques, F.; De Almeida, R.F.M.; Mendes, F.; Enyedy, É.A.; Santos, I.; Pessoa, J.C.; Kiss, T.; Garcia, M.H. [RuII(η5-C5H5)(bipy)(PPh3)]+, a promising large spectrum antitumor agent: Cytotoxic activity and interaction with human serum albumin. *J. Inorg. Biochem.*, **2012**, *117*, 261-269.
- [38] Morais, T.S.; Silva, T.J.L.; Marques, F.; Robalo, M.P.; Aveçilla, F.; Madeira, P.J.A.; Mendes, P.J.G.; Santos, I.; Garcia, M.H. Synthesis of organometallic ruthenium(II) complexes with strong activity against several human cancer cell lines. *J. Inor. Biochem.*, **2012**, *114*, 65-74.
- [39] Fotakis, G.; Timbrell, J.A. *In vitro* cytotoxicity assays: Comparison of LDH, neutral red, MTT and protein assay in hepatoma cell lines following exposure to cadmium chloride. *Toxicol. Lett.*, **2006**, *160* (2), 171-177.
- [40] Azar, H.A.; Hansen, C.T.; Costa, J.N. NIH(S)II-nu/nu mice with combined immunodeficiency: A new model for human tumor heterotransplantation. *J. Nat. Cancer Inst.*, **1980**, *65*(2), 421-430.
- [41] Yen, W.C.; Lamph, W.W. The selective retinoid X receptor agonist bexarotene (LGD1069, Targretin) prevents and overcomes multidrug resistance in advanced breast carcinoma. *Mol. Cancer Therapeut.*, **2005**, *4*(5), 824-834.
- [42] Huang, F.; Mazin, A.V. A small molecule inhibitor of human RAD51 potentiates breast cancer cell killing by therapeutic agents in mouse xenografts. *PloSone* **2014**, *9*(6), e100993.
- [43] Roodhart, J.M.; Daenen, L.G.; Stigter, E.C.; Prins, H.J.; Gerrits, J.; Houthuijzen, J.M.; Gerritsen, M.G.; Schipper, H.S.; Backer, M.J.; Van A.M.; Vermaat, J.S.; Moerer, P.; Ishihara, K.; Kalkhoven, E.; Beijnen, J.H.; Derksen, P.W.; Medema, R.H.; Martens, A.C.; Brenkman, A.B.; Voest, E.E. Mesenchymal stem cells induce resistance to chemotherapy through the release of platinum-induced fatty acids. *Cancer Cell*, **2011**, *20*(3), 370-383.
- [44] Scolaro, C.; Geldbach, T.J.; Rochat, S.; Dorcier, A.; Gossens, C.; Bergamo, A.; Cocchietto, M.; Tavernelli, I.; Sava, G.; Rothlisberger, U.; Dyson, P.J. Influence of hydrogen-bonding substituents on the cytotoxicity of RAPTA compounds. *Organometallics*, **2006**, *25*(3), 756-765.
- [45] Webb, M.I.; Walsby, C.J. Control of ligand-exchange processes and the oxidation state of the antimetastatic Ru(III) complex NAMI-A by interactions with human serum albumin. *Dalton transactions (Cambridge, England : 2003)* **2011**, *40*(6), 1322-1331.
- [46] Morais, T.S.; Santos, F.C.; Corte-Real, L.; Garcia, M.H. Exploring the effect of the ligand design on the interactions between [Ru(eta5-C5H5)(PPh3)(N,O)][CF3SO3] complexes and human serum albumin. *J. Inorg. Biochem.*, **2013**, *129*, 94-101.
- [47] Beckford, F.; Thessing, J.; Woods, J.; Didion, J.; Gerasimchuk, N.; Gonzalez-Sarrias, A.; Seeram, N.P. Synthesis and structure of [(eta(6)-p-cymene)Ru(2-anthracen-9-ylmethylene-N-ethylhydrazinecarbothioamide)Cl] Cl; biological evaluation, topoisomerase II inhibition and reaction with DNA and human serum albumin. *Metallomics. Integ. Biomet. Sci.*, **2011**, *3*(5), 491-502.
- [48] Beckford, F.A. Reaction of the anticancer organometallic ruthenium compound, [(η(6)-p-Cymene)Ru(ATSC)Cl]PF(6) with Human Serum Albumin. *Int. J. Inorg. Chem.*, **2010**, *2010*(975756), 1-7.

- [49] Westermann, B. Molecular machinery of mitochondrial fusion and fission. *J. Biolog. Chem.*, **2008**, *283*(20), 13501-13505.
- [50] Martin, S.J.; Reutelingsperger, C.P.; McGahon, A.J.; Rader, J.A.; Van Schie, R.C.; LaFace, D.M.; Green, D.R. Early redistribution of plasma membrane phosphatidylserine is a general feature of apoptosis regardless of the initiating stimulus: Inhibition by overexpression of Bcl-2 and Abl. *J. Exp. Med.*, **1995**, *182*(5), 1545-1556.
- [51] Vermes, I.; Haanen, C.; Steffens-Nakken, H.; Reutelingsperger, C. A novel assay for apoptosis. Flow cytometric detection of phosphatidylserine expression on early apoptotic cells using fluorescein labelled Annexin V. *J. Immunolog. Method.*, **1995**, *184*(1), 39-51.
- [52] Bielawski, K.; Czarnomysy, R.; Muszynska, A.; Bielawska, A.; Poplawska, B. Cytotoxicity and induction of apoptosis of human breast cancer cells by novel platinum(II) complexes. *Environ. Toxicol. Pharmacol.*, **2013**, *35*(2), 254-264.
- [53] Grimm, H.; Finney, D.J. Statistical method in biological assay. 3. ed. Charles Griffin & Co., London and High Wycombe 1978. VII, 508 S., £ 19 net. *Biometrical. J.*, **1979**, *21*(7), 689-690.
- [54] Lang, J.Y.; Chen, H.; Zhou, J.; Zhang, Y.X.; Zhang, X.W.; Li, M. H.; Lin, L.P.; Zhang, J.S.; Waalkes, M.P.; Ding, J. Antimetastatic effect of salvicine on human breast cancer MDA-MB-435 orthotopic xenograft is closely related to Rho-dependent pathway. *Clin. Cancer Res.*, **2005**, *11*(9), 3455-3464.
- [55] Zhang, J.; Bera, T.K.; Liu, W.; Du, X.; Alewine, C.; Hassan, R.; Pastan, I. Megakaryocytic potentiating factor and mature mesothelin stimulate the growth of a lung cancer cell line in the peritoneal cavity of mice. *PLoS One* **2014**, *9*(8), e104388.